Arul Periyanayagam. et al., / Vol. 02 / Issue 04 / 2014 / 251 – 258.

Research Article

Available Online at: www.ijphr.com

International Journal of Pharmaceuticals and Health care Research

ISSN: - 2306 – 6091

DISSIPATED POWER EFFECT DUE TO AERIAL RESISTIVE HEATING ON E- TO H-MODE TRANSITION IN INDUCTIVELY JOINED OXYGEN PLASMA

*Arul Periyanayagam, Teweldebrhan Gebru

Department of Physics, College of Natural and Computational Sciences,
University of Gondar, Post Box No. 196, Ethiopia.

Abstract

The problem of the effective power input into plasma is investigated for the inductively coupled RF oxygen discharge operated at 13.56 MHz. The power significantly deviates especially at the E- to H-mode transition. In order to enlighten this phenomenon the U–I characteristics of the discharge are recorded. With these data, we have recalculated the power deposited into plasma and determined the effective power losses due to the resistive antenna heating. The E–H mode transition is investigated in the pressure range from 10 to 200 Pa. With an increase of the working gas pressure, the threshold for the E–H transition moves towards the higher powers. The transition exhibits a hysteresis for the pressures higher than 10 Pa. When the dissipated power due to the antenna resistive heating is taken into account, the characteristic hysteresis profile skews towards lower power as compared to the case of taking generator power as a relevant parameter. This means that the E-mode is strongly affected by the way the power is obtained, while for the H-mode the generator power can be considered as a relatively good external parameter.

Keywords: Oxygen, Inductively joined plasma, Mode transitions, Discharge power.

Received on- 15.12.2014 ; Revised and accepted on- 27.12.2014; Available online- 30.12.2014

Introduction

Modern plasma processing systems often contain a combination of two or more capacitively (CCP) and/or inductively coupled (ICP) multi-frequency plasma reactors. The complex designs are introduced to provide independent control of important etching parameters like ion energies and charged particle concentrations in order to achieve high aspect ratios with minimum damage to the device.[1–3] The complexity of plasma systems made plasma diagnostics very challenging, due to multi-parameter control. High chemical reactivity of non-thermal plasma is exploited for processing of materials like polymers, composites, textiles, and for biomedical applications.[3–16]

Inductively coupled plasma reactors operate in two regimes. The E-mode is sustained at lower powers and is characterized by low electron densities but high mean electron energies with non-equilibrium distribution. In the
H-mode, the electron densities are high, while mean electron energy is lower.

A special feature of mode transition is the hysteresis[2]. ICP is usually initiated locally by the capacitive coupling between the RF coil and surroundings, known as E-mode. Next, electrons are accelerated in induced electric field, which results from oscillating magnetic field inside the

Author for Correspondence:
Arul Periyanayagam
E-mail: abisuabi@yahoo.co.in

coil (H-mode) providing the power given by the RF power supply is large enough. There is always a threshold power or induced voltage below, which no H-mode can be formed. Hysteresis occurs as the transition back to the E-mode at a lower power/ induced voltage. This effect is observed in plasmas sustained at different frequencies (13.56 MHz[17, 18], 0.56 MHz[19] and 0.5 MHz[20]).

The difference in modes can in principle be observed from electrical properties [deposited power, Volt-Ampere (U–I) characteristics][19–23] and plasma brightness (or measurements of densities of excited states).[17, 18, 24] Besides the optical emission spectroscopy (OES), where the significant difference of line intensities is recorded for the two modes. The transition of modes is also easily detectable by using Langmuir probes to record the changes in electron densities and/or electron temperature.[25, 26] Mode transitions are mostly reported in noble gases. The transition between two modes is studied using different types of diagnostics, but recently the most useful results may be obtained by observing 2D emission profiles, which reveal directly difference between the two modes.[27, 28]

Recent measurements on oxygen plasma have been reported.[29] The increase in atomic oxygen concentrations has been recorded during the transition from E- to H-mode,[30] where an increase of the factor of 3 has been reported at elevated pressure (160 Pa). A key and relevant external parameter has been proven to be a generator power. In most studies of E–H transition power measured at the power supply is used. Sometimes reflected power is subtracted. However, for the more complete understanding of the observed phenomena (E–H transition power and hysteresis effect) it is necessary to include other losses, such as the power emitted by the radio waves and the heating of the coil due to the resistance.

In this paper, we study the effects of dissipated power due to antenna resistive heating on the E–H mode transition and the hysteresis effect. We also discuss in details the power efficiency during the mode transition in oxygen plasma in both directions (E–H and H–E). We unfold the influence of the coil/reactor wall temperature on the dissipated power, measure, calculate and compare effective power losses in the RF coil. Furthermore, we define the regions, where plasma does not operate in a stable regime and elaborate on hysteresis effect.[21] Commercial current and voltage probes and the procedure for the determination of the plasma power and electrical properties of the system can be applied to complex plasma processing systems as well. Herein we present also results of electrical properties of the discharge.

Experimental details

Experimental set-up of the ICP reactor was used in the experiments as presented in Fig. 1. The system was composed from an RF power supply (Dressler CESAR 1312D), matching box and discharge tube made of Pyrex. The discharge tube was 80 cm long with the diameter of 4 cm. The pressure in the reactor was measured by an absolute pressure transducer MKS Baratron 722A positioned at the chamber gas outlet. The experimental vessel was evacuated using a two-stage oil rotary pump with an ultimate pressure of approximately 0.5 Pa. After evacuating the vacuum chamber to the base pressure, oxygen feedstock gas was continuously let into the chamber.

Plasma glow discharge was created by an inductively coupled RF generator that operates at 13.56 MHz with maximum output power of 1,200 W. The L-type matching network was employed with two vacuum variable tuning capacitors, C1 = 5–500 pF and C2 = 5–500 pF and was connected directly to the inductive coil to reduce resistive losses. The capacitors were tuned to achieve the minimal value of the reflected power, while plasma was operated in the H-mode. The values were kept constant throughout the measurements. Power supply was coupled to the discharge by a coil (six turns) made of copper. The applied power was recorded as the difference between the forward and reflected power as read from the power supply meter. IR-pyrometer Raytek Raynger MX4+ was used to measure the temperature and determine the heat loss in the coil. After a certain period of plasma operation the temperature increased and became close to the melting temperature of the glass chamber. Therefore, coil and the discharge area had to be air cooled during all the measurements in order to prevent the overheating. Besides the temperature measurements, we used commercial current and voltage probes (Tektronix A6302, Tektronix P6015A) in order to obtain current and voltage characteristic. Oxygen was

used as a feeding gas in the pressure range from 10 to 200 Pa. Power used to create discharge by RF power supply was varied in small increments and characteristics were measured between 10 and 1,000 W.

Results and discussion

We now discuss the influence of the antenna resistive heating on power transmission, stable regimes of plasma operation, power transfer efficiency, Volt-Ampere characteristics of the discharge and hysteresis effect of E- and Hmode transitions. Finally, we compare the results, when the generator power is used as a relevant parameter with the results obtained in this study, when the power dissipation is taken into account.

Coil heating can significantly influence the transmission efficiency of the power given by the power supply to the discharge. In order to determine the heat loss in the coil, we have measured the temperature and the power dissipated as the heat loss has been calculated. During temperature measurements, we have implied no coil cooling with convective air or running water. The temperature dependence of the coil after plasma ignition is presented in Fig. 2 for the case of RF power supply at 500 W and operating pressure 50 Pa. The coil temperature behavior typically shows two regimes characterized by different slopes of temperature versus time. At first, the temperature of the coil increases with the time only due to resistive heating. However, after a certain period of time, the temperature curve steepens probably due to the heating coming from the discharge itself, which starts to heat up chamber walls. The position of the inflection point depends on the pressure and the power input by the power supply. At higher powers and lower pressures the heating due to the ignited discharge is more pronounced as compared to the lower powers and/ or higher pressures.

The power dissipated in the coil is shown in Fig. 3. It is calculated as Pdiss = m.cCu.dT/dt, where m is coil mass, cCu is specific heat coefficient for copper and dT/dt is the slope of the first part of the temperature curve, due to the resistive heating, as shown in Fig. 2. At 30 Pa, dissipated power does not change with forward power. For 50 Pa the dissipated power increases linearly with forward power, where the dissipation at 700 W is about 8 W. Since there is an additional constant heating coming from discharge, the temperature of the coil as well as the glass chamber itself increases linearly with time. At the same time, the overheating of the discharge area leads to the decrease in power transmission efficiency.

Besides the influence of resistive antenna heating on power transmission, the transition from E- to H-mode is clearly visible as a decrease in reflected power, as shown in Fig. 4. Threshold point (forward power where transition occurs) for the E- to H-mode transition moves towards higher powers with an increase of working gas pressure. However, at 200 Pa we do not observe this threshold point because at this pressure the transition is out of the power range of our RF power supply. In order to observe this transition, we would need forward power higher than 800 W. All power–pressure dependences show ‘the gaps’ in the power range, where no stable discharge can be obtained. This occurs due to the unstable transition between the two modes of operation. Even more so, in this range, we have significant power oscillations. These oscillation areas are marked in Fig. 4 for pressures of 40 and 100 Pa with red and green shaded area, respectively. The range of power oscillations, where no stable discharge could be obtained, becomes wider when increasing the working pressure.

The applied power Pa is determined as the difference between the forward and reflected power. Both are measured by the RF power supply meter. The resolution of the RF generator power meter is±1 W. In order to determine the ‘‘real’’ power transmitted to the plasma, we need to determine the effective power losses in the antenna. The effective power loss is calculated as I^2Reff, where Reff represents the resistance in the antenna and associated hardware.[20, 31, 32] The effective coil resistance is determined from dissipating a known power in the matching circuit with no plasma present. Based on the power dissipated in the matching circuit and the current, the effective coil resistance has been measured to be 0.05Ωduring the reported measurements. From the obtained value, lower than 0.1Ω, we could assume that the coupling efficiency of the system is very good and above 90 % for most of the used discharge parameters.[33]

Plasma power is then determined as

$$P_p = P_a - I^2 R_{eff}, \quad \text{(Eq. 1)}$$

Where, I is the RMS current flowing in the circuit and Reff is the effective resistance of the coil and associated hardware. Here it should be noted that if the plasma significantly alters the current distribution in the chamber, then Reff and the power transmitted into the plasma would change. Reff can be calculated using the resistivity of copper (qCu = 1.59 x 10^{-8} Ω m), the theoretical skin depth of 13.56 MHz current in the conductors (δ = 18 μm) at the given length (l = 0.91 m) and circumference (O = 0.14 m) of the six-turn coil with interconnects:

$$R_{eff} = \rho_{Cu} \cdot \frac{l}{O \cdot \delta} = 0.006\ \Omega \quad \text{(Eq. 2)}$$

However it is worth noting that this effective resistance does not include contributions from the tuning capacitors. In order to calculate Reff, we also need to assume that the current distribution around the cross section circumference of the coil is uniform. More realistic situation of the non-uniform current distribution leads to an increase in effective resistance. Eq. (2) gives only the lower bound of the actual resistance, so in further analysis the experimentally obtained value of resistance has been used.

The measured power transfer efficiency Pp/Pa is presented in Fig. 5 as a function of applied power. The power transfer efficiency rises steeply from about 75 % in E-mode to a nearly constant efficiency in H-mode, with values from 95 to 98 % at different pressures. We have not observed the E–H mode transition at 200 Pa, due to the limitations of the power supply. For lower pressures, the power transfer efficiency rises faster than for higher pressures. At lower pressures, the maximal power efficiency is reached at lower applied powers. Moreover, at high pressures, the transition to H-mode can be expected at higher applied power values.

It is interesting to note how the coil current behaves at different pressures. From Fig. 6, we observe that the decrease of the pressure increases the current significantly, especially for the H-mode. This occurs due to the increase of the electric field and therefore the increase of the RF magnetic flux. At the same time, at 100 W, the current is almost constant throughout the measured pressure range, when the discharge is in the E-mode.

The E–H transition is also clearly seen from the U–I characteristics of the discharge presented in Fig. 7. When the discharge is in the E-mode, RMS values of the voltage linearly increase up to the threshold values, where transition occurs. After the transition, RMS values of voltage drop suddenly and again start to increase with the increase of the power transmitted into the plasma. In our discharge, RMS values of the voltage are in the range between 200 and 1250V, whereas the RMS values of current lie in the range 2.5–20 A. After the transition (inflection point), the RMS voltage still increases, but in a slower manner compared to the previous E-mode. Two distinct slopes show the change of the effective plasma impedance. In the E-mode, the slope is steeper leading to the conclusion that the plasma impedance is higher than in the H-mode.

The transition between E- and H-modes has already been reported to exhibit hysteresis.[17–19, 31] The threshold power for H to E transition is normally lower than in the case of E to H transition. Plasma stays in the H-mode even for lower powers, when applied power is decreased. Several authors[19, 21] have suggested that this threshold point for the H-mode and the hysteresis originates from the electron energy balance in the discharge. It is necessary that the power absorbed by the electrons is balanced by the power dissipated in the discharge for a stable discharge to exist (both E- and H-mode). To obtain the transition between the two modes, we need to assume a nonlinearity in the power absorbed or dissipated in the plasma.[34] RMS voltages are presented in Fig. 8, as a function of the power deposited into the ICP plasma for (a) 10 Pa, (b) 20 Pa and (c) 40 Pa in Fig. 8. At the lowest pressure of 10 Pa, the effect of hysteresis is minimal. However, when we increase the working pressure, the hysteresis becomes more pronounced, as in the case of 40 Pa, as shown in Fig. 8(c).

In most of the cases, the hysteresis is demonstrated as a function of the generator power. However, Fig. 9 clearly demonstrates that if the antenna dissipated power due to the resistive heating and the generator

reflected power are taken into account the hysteresis skews and slightly shifts towards lower power.

The change in the shape profile shows that the recalculated power is strongly affecting the E-mode. If the generator power is taken as a relevant external parameter, the E- to H-mode transition occurs in only a few watt span in the power. On the other hand, if the dissipated and reflected power is included, the E- to H-mode is having a power span of several hundred watts. Unlike the E-mode, the H-mode is only slightly affected by the way the power is determined. While outside the realm of our facilities, spatial profiles of negative ions in E and H modes cannot be easily measured for our experiment and should be sought from plasma modelling. It is also known that the negative ion energies are far less than those of electrons. However, electrons need to gain enough energy to produce the excited states that are observed in measurements. In addition to the negative ions, density of excited states such as oxygen metastables also plays an enhanced role in the transition from E to H.

Conclusions

This paper presents the power measurements, electrical characterization and plasma behavior obtained in an inductively coupled RF oxygen discharge that operates at 13.56 MHz. We include the effects of dissipated power due to the resistive antenna heating (together with the generator reflected power) and study the E- to H-mode transition and its hysteresis effect. Furthermore, we compare the results in two cases: when generator power is used as a relevant external parameter and when the recalculated so called ‘‘plasma power’’ is used. We find that if the power dissipation is taken into account the difference in the power values is pronounced for the E-mode. In the case of H-mode, the generator power can be considered as a satisfactory parameter.

We also investigate transition from the low density capacitive E-mode to the inductive H-mode for the range of pressures from 10 to 200 Pa. We find that the increase in the working gas pressure requires higher powers deposited into plasma in order to observe the mode transition. Moreover, in all mode transitions the oscillations of discharge occur. This is explained by a rapid change in plasma density and topography during E–H transition, which results in an unstable plasma system. The power transfer efficiency is in the range of 70–85 % for the E-mode, whereas it is much higher and constant for the H-mode (~95 %). Additionally, the hysteresis effects have to be accounted for when the pressure is above 10 Pa, since the transition point is significantly shifted. All of these have to be taken into account when reporting power input into plasma during material processing, but is mostly unaccounted for in scientific reports.

References

1. M A Lieberman and A J Lichtenberg Principles of plasma discharge and materials processing (Hoboken: Wiley) (2005)
2. T Makabe and Z L Petrovic´ Plasma electronics: applications in microelectronic device fabrication (New York: Taylor and Francis) (2006)
3. U Cvelbar et al. Appl. Surf. Sci. 253 8669 (2007)
4. U Cvelbar, S Pejovnik, M Mozetic and A Zalar Appl. Surf. Sci. 210 255 (2003)
5. B Denis, S Steves, E Semmler, N Bibinov, W Novak and P Awakowicz Plasma Process. Polym. 9 619 (2012)
6. V Ilic et al. Ind. Eng. Chem. Res. 49 7287 (2010)
7. M Laroussi Plasma Process. Polym. 2 391 (2005)
8. D Mihailovic´ et al. Cellulose 18 811 (2011)
9. N Puacˇ, Z Lj Petrovic´, S Zˇ ivkovic´, Z Giba, D Grubisˇic´ and A Đord evic´ Plasma Process. Polym. (Weinheim: WILEY-VCH Verlag GmbH & Co. KGaA) Chapter 15 p 193 (2005)
10. N Puacˇ et al. J. Phys. D Appl. Phys. 39 3514 (2006)
11. M Modic, I Junkar, A Vesel and M Mozetic Surf. Coat. Technol. 213 98 (2012)
12. J Vasiljevic´ et al. Cellulose 20 277 (2012)
13. Z Persˇin, M Devetak, I Drevensˇek-Olenik, A Vesel, M Mozetic and K Stana-Kleinschek Carbohydr. Polym. 97 143 (2013)
14. K H Karstensen et al. Environ. Sci. Policy 9 577 (2006)
15. G Mandal and T Ganguly Indian J. Phys. 85 1229 (2011)
16. A Kaplan, H Bu¨yu¨kuslu, E Tel, A Aydin and M H Bo¨lu¨kdemir Indian J. Phys. 85 1615 (2011)

17. U Kortshagen, N D Gibson and J E Lawler J. Phys. D Appl. Phys. 29 1224 (1996)
18. Y Miyoshi, Z L Petrovic and T Makabe J. Phys. D Appl. Phys. 35 454 (2002)
19. I M El-Fayoumi, I R Jones and M M Turner J. Phys. D Appl. Phys. 31 3082 (1998)
20. K N Ostrikov, S Xu and M Y Yu J. Appl. Phys. 88 2268 (2000)
21. K Suzuki, K Nakamura, H Ohkubo and H Sugai Plasma Sources Sci. Technol. 7 13 (1998)
22. G Cunge, B Crowley, D Vender and M M Turner Plasma Sources Sci. Technol. 8 576 (1999)
23. N Nimje, S Dubey and S Ghosh Indian J. Phys. 84 1567 (2010)
24. Y C Wang, E C Benck, M Misakian, M Edamura and J K Olthoff J. Appl. Phys. 87 2114 (2000)
25. S Xu, K N Ostrikov, WLuo and S Lee J. Vac. Sci. Technol. A 18 2185 (2000)
26. Y Chen, Z G Guo, X M Zhu, Z G Mao and Y K Pu J. Phys. D Appl. Phys. 40 5112 (2007)
27. Y Hayashi, Y Mitsui, T Tatsumi and T Makabe New J. Phys. 13 073025 (2011)
28. M Satoshi, H Yuichiro and M Toshiaki Plasma Sources Sci. Technol. 19 055007 (2010)
29. M Zaka-Ul-Islam, K Niemi, T Gans and D O'Connell Appl. Phys. Lett. 99 041501 (2011)
30. R Zaplotnik, A Vesel and M Mozetic EPL 95 55001 (2011)
31. A M Daltrini, S A Moshkalev, T J Morgan, R B Piejak and W G Graham Appl. Phys. Lett. 92 061504 (2008)
32. P A Miller, G A Hebner, K E Greenberg, P D Pochan and B P Aragon J. Res. Natl. Inst. Stan. 100 427 (1995)
33. J Hopwood Plasma Sources Sci. Technol. 3 460 (1994)
34. M M Turner and M A Lieberman Plasma Sources Sci. Technol. 8 313 (1999)

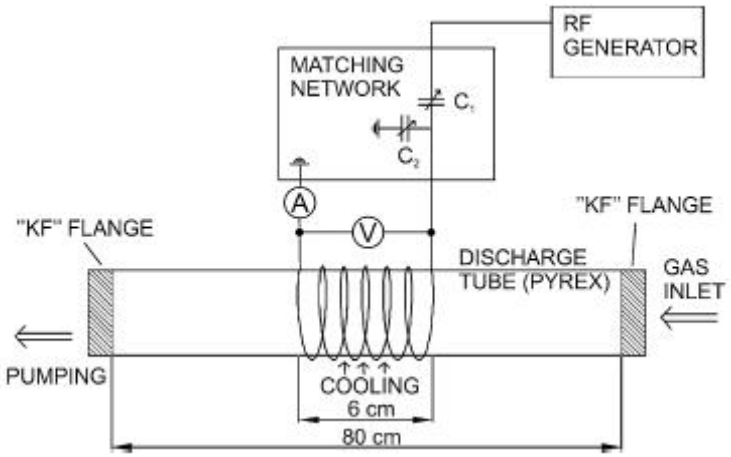

Fig. No. 01: Experimental set-up for the ICP RF discharge

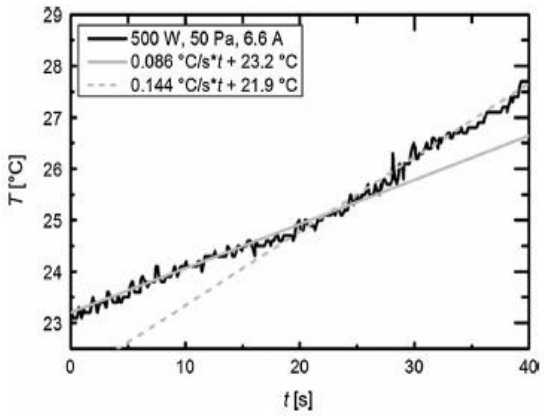

Fig. No. 02: Time dependence of the coil temperature after the plasma ignition

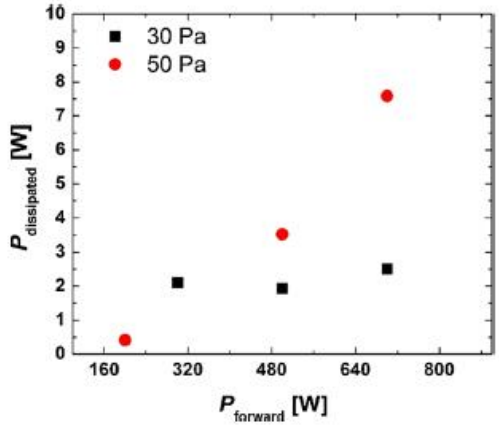

Fig. No. 03: Power dissipated as coil heating for two different pressures while plasma was ignited

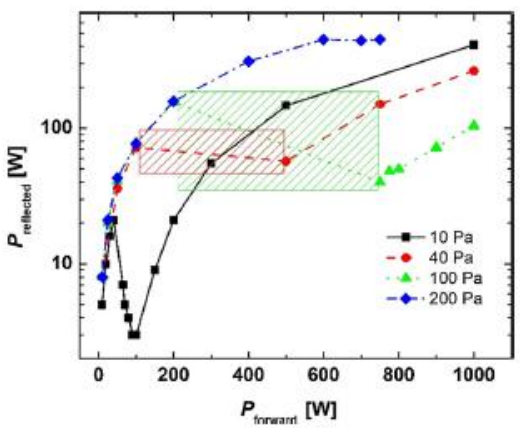

Fig. No. 04: Dependence of the reflected power for different pressures on forward power of the RF power supply

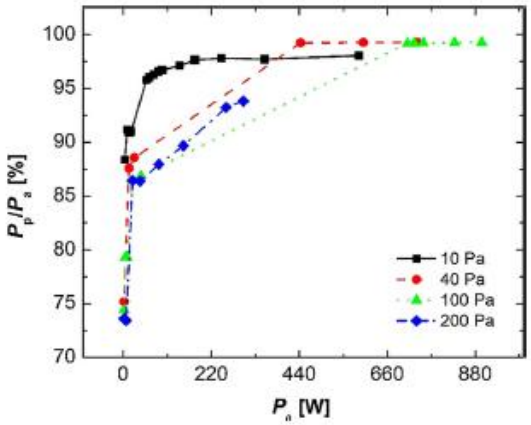

Fig. No. 05: Power transfer efficiency for four different pressures shown as a function of applied power

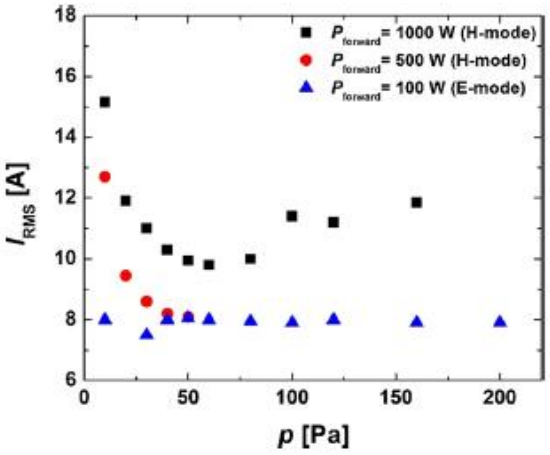

Fig. No. 06: RMS current values shown as a function of working pressure

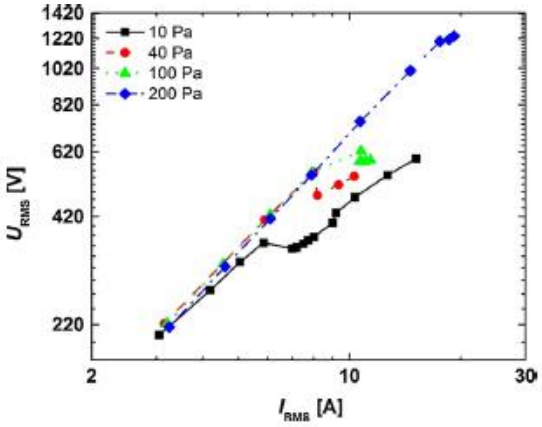

Fig. No. 07: Urms – Irms characteristics of the discharge

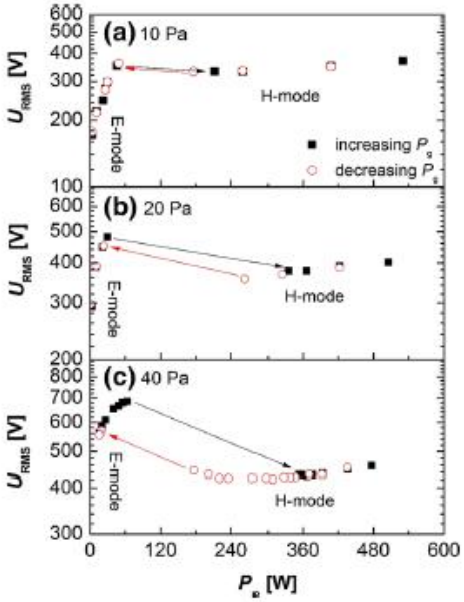

Fig. No. 08: Dependence of the Urms values on the power deposited to the plasma for different pressures: (a) 10 Pa, (b) 20 Pa, (c) 40 Pa. Measurements were made for an increase of the power given by RF power supply (increasing Pg) and after that, a decreasing power (decreasing Pg) in order to detect hysteresis

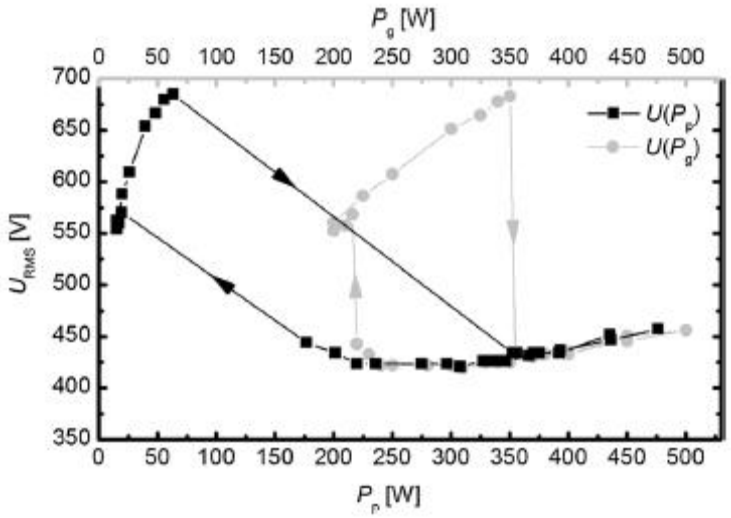

Fig. No. 09: Influence of the resistive antenna heating on the hysteresis for E- and H-mode at 40 Pa (generator power vs. plasma power)